Postprint of: Eremeyev V.A., Turco E., Enriched buckling for beam-lattice metamaterials, Mechanics Research Communications, Vol. 103 (2020), 103458, DOI: 10.1016/j.mechrescom.2019.103458

Enriched buckling for beam-lattice metamaterials

Victor A. Eremeyev [a], Emilio Turco [b,*]

[a] Faculty of Civil and Environmental Engineering, Gdańsk University of Technology, ul. Gabriela Narutowicza 11/12, Gdańsk 80-233, Poland
[b] Department of Architecture, Design and Urban Planning, University of Sassari, via Garibaldi 35, Asilo Sella, Alghero (SS) 07041, Italy

A B S T R A C T

We discuss two examples of beam-lattice metamaterials which show attractive mechanical properties concerning their enriched buckling. The first one considers pantographic beams and the nonlinear solu- tion is traced out numerically on the base of a Hencky's model and an algorithm based on Riks' arc-length scheme. The second one concerns a beam-lattice with sliders and the nonlinear solution is discussed in analytic way and, finally, extended to the case of uniform in-plane tension. Some concluding remarks draw possible future developments and challenges.

Keywords:
Beam-lattice
Pantographic lattice
Stability
Sliders

1. Introduction

Nowadays beam-lattice materials are widely used in civil, mechanical and aerospace engineering, see, *e.g.*, [1–5]. As their structure mimics crystalline lattices and their properties, see *e.g.* [6–9], these materials have very promising characteristics such as, *e.g.*, a light weight with relatively high stiffness, flexibility, acoustic response, thermal insulation. In particular, such lattice structures, *e.g.* auxetics, demonstrate unusual mechanical property, *e.g.* a negative Poisson ratio [10,11]. When beam-lattice structures are homogenized they might convert into their continual counterpart the mechanical behaviour shown in the discrete model. Homogenized model deriving from beam-lattice structures could be a kinematically enriched medium as, *e.g.*, Cosserat continuum, micromorphic or strain gradient media, see [12–17].

High flexibility of the beam-lattice metamaterials may results in the loss of stability as in the case of rods, beams, and frames, see, *e.g.*, [18–21]. In particular, the buckling of struts in elastomer open-cell foams leads to softening behaviour in a loading curve [1]. Instability for certain metamaterials are also discussed in [3,22,23]. On the other hand an enriched kinematics of beam-lattice metamaterials may lead to more complex buckling behaviour than in the case of classic structural mechanics.

In order to demonstrate possible complex buckling behaviour of beam-lattice metamaterials we consider here two examples. The first one concerning the so-called pantographic beam structures, see [13,16], will be discussed in Section 2. Here we consider the Euler type instability for a beam-like pantographic structure and discuss its difference from the classic case. In Section 3 we consider beam-lattices with sliders under tension as a second example of unusual behavior. Recently, elastic systems with sliding interfaces under tensile forces were discussed in [24,25]. Some concluding remarks, Section 4, close the paper and anticipate some possible future developments.

2. Pantographic beam

We consider the straight pantographic beam reported in Fig. 1 where we distinguish two families of extensional-bending bars connected in their midpoints by torsional links. By limiting the analysis to the in-plane behaviour, it has been proven in several papers, see [26–31], that this system can be modeled by an assembly of extensional and rotational springs such as those reported again in Fig. 1. The Hencky's model is completely defined by the strain energy of each one elastic spring, in formulae

$$\begin{aligned}
\mathcal{E}_a &= \frac{1}{2}a\Delta\ell^2\,,\\
\mathcal{E}_b &= b(1+\cos\beta)\,,\\
\mathcal{E}_c &= \frac{1}{2}c\left(\gamma-\frac{\pi}{2}\right)^2\,,\\
\mathcal{E}_d &= d\left(1-\cos\left(\delta-\frac{\pi}{4}\right)\right)\,,
\end{aligned} \tag{1}$$

being $\mathcal{E}_a$, $\mathcal{E}_b$ and $\mathcal{E}_c$ the strain energies stored in extensional, bending and shearing springs, see again Fig. 1; the strain energy $\mathcal{E}_d$ is related to rotational springs on the left and right ends of the pantographic beam. The stiffnesses *a, b, c* and *d* of above mentioned

* Corresponding author.
E-mail address: emilio.turco@uniss.it (E. Turco).

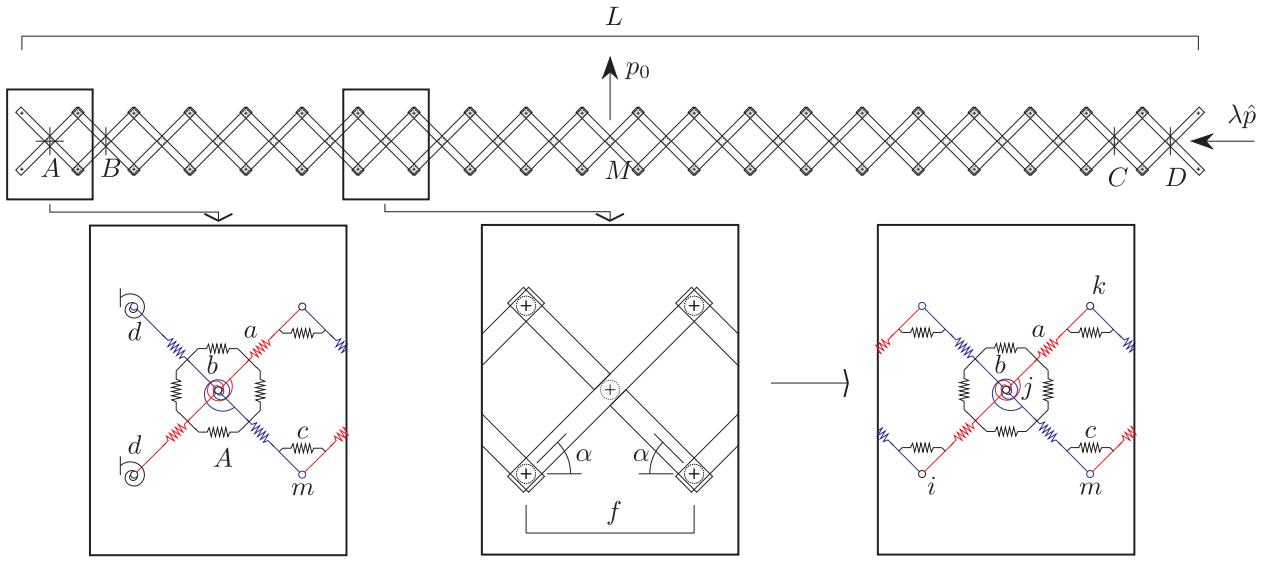

Fig. 1. Geometry, loads and Hencky's model of a pantographic beam in the case $\alpha = \pi/4$ under compression load $\lambda\hat{p}$ and imperfection load p_0 (displacement of points *A*, as well as vertical displacements of points *B*, *C* and *D*, are set to zero.

springs and the associated strain measures $\Delta\ell$ (stretching), $\cos\beta$ (bending), γ (shearing) and δ (rotation), defined as functions of the current positions of nodes of the pantographic beam, complete the definition of the strain energy of each one elastic spring

$$\Delta\ell = \|p_j - p_i\| - \|P_j - P_i\|\,,$$
$$\cos\beta = \frac{\|p_j - p_i\|^2 + \|p_k - p_j\|^2 - \|p_k - p_i\|^2}{2\|p_j - p_i\|\|p_k - p_j\|}\,,$$
$$\gamma = \arccos\frac{\|p_j - p_m\|^2 + \|p_k - p_j\|^2 - \|p_k - p_m\|^2}{2\|p_j - p_m\|\|p_k - p_j\|}\,,$$
$$\cos\left(\delta - \frac{\pi}{4}\right) = \frac{\mathbf{v}\cdot\mathbf{e}_1 + \mathbf{v}\cdot\mathbf{e}_2}{\|P_j - P_i\|^2}\,, \tag{2}$$

where P_i and p_i are the reference and the current position of the i-th node (the same is true for nodes j, k and m), respectively, $\mathbf{v} = (p_j - p_i) - (P_j - P_i)$ and $\mathbf{e}_1$, $\mathbf{e}_2$ are the horizontal and vertical unit vectors.

The nonlinear system of equilibrium equations, obtained by enforcing the stationarity condition for the potential energy with respect to the vector of nodal displacements $\mathbf{u}$, can be written as

$$\mathbf{s}[\mathbf{u}] - \mathbf{p}[\lambda] = \mathbf{0}\,, \tag{3}$$

being $\mathbf{s}$ the structural reaction vector, depending upon displacements $\mathbf{u}$, and $\mathbf{p}[\lambda]$ the vector of external loads described as a function of the dimensionless load parameter λ. The reaction $\mathbf{s}$ is defined, starting from the strain energy $\mathcal{E}$ of the system, as

$$\mathbf{s} = \frac{\mathrm{d}\mathcal{E}}{\mathrm{d}\mathbf{u}}\,, \tag{4}$$

and the loads are expressed in the form

$$\mathbf{p}[\lambda] = \mathbf{p}_0 + \lambda\hat{\mathbf{p}}\,, \tag{5}$$

in such a way that we can distinguish loads in a part, $\mathbf{p}_0$, independent from the dimensionless parameter λ (that can be used to model the so-called imperfections) and a part, $\lambda\hat{\mathbf{p}}$, linearly increasing with the dimensionless parameter λ.

The solution of the nonlinear system of equations (3) can be achieved by using a step-wise procedure based on Newton's method. If the pair $(\mathbf{u}_i, \lambda_i)$ – the index i refers to the considered iteration – represents an equilibrium point, we can estimate the next, and nearby, equilibrium point $(\mathbf{u}_i + \Delta\mathbf{u}, \lambda_i + \Delta\lambda)$ by linearizing Eq. (3)

$$\mathbf{s}[\mathbf{u}_i] + \mathbf{K}\Delta\mathbf{u} - \left(\mathbf{p}_0 + (\lambda_i + \Delta\lambda)\hat{\mathbf{p}}\right) \approx \mathbf{0}\,, \tag{6}$$

being the stiffness matrix $\mathbf{K}$ defined as

$$\mathbf{K} = \frac{\mathrm{d}\mathbf{s}}{\mathrm{d}\mathbf{u}}\,, \tag{7}$$

and computed in $\mathbf{u}_i$. Newton's method is based on linearization (6) that gives

$$\Delta\mathbf{u} = -\Delta\lambda\mathbf{K}^{-1}\hat{\mathbf{p}}\,. \tag{8}$$

Unfortunately, the Newton's method fails when $\mathbf{K}$ is singular or nearly-singular, *e.g.* in or near to limit points of the equilibrium path, *i.e.* the stiffness matrix is positive semi definite. In order to go around this limitation, Riks [32] proposed to reconstruct the equilibrium path by parameterizing this curve by its arc-length instead than the dimensionless load parameter λ. In this way, the resulting integration scheme bypass the lack of convergence in the neighborhood of limit points. Obviously, Riks' method requires an additional equation to balance the number of unknowns. More specifically, Riks' arc-length scheme is based on a correction on the Newton's extrapolation (8). Starting from an equilibrium point $(\mathbf{u}_i, \lambda_i)$, we can compute the Newton's extrapolation $(\Delta\mathbf{u}, \Delta\lambda)$ and the successive correction $(\dot{\mathbf{u}}, \dot{\lambda})$. The pair $(\dot{\mathbf{u}}, \dot{\lambda})$ can be computed from the linearization

$$\mathbf{s}[\mathbf{u}_i + \Delta\mathbf{u}] + \mathbf{K}\dot{\mathbf{u}} - (\mathbf{p}_0 + (\lambda_i + \Delta\lambda + \dot{\lambda})\hat{\mathbf{p}}) \approx \mathbf{0}\,, \tag{9}$$

from which we can evaluate $\dot{\mathbf{u}}$ as

$$\dot{\mathbf{u}} = -\mathbf{K}^{-1}\left(\mathbf{s}[\mathbf{u}_i + \Delta\mathbf{u}] - (\mathbf{p}_0 + (\lambda_i + \Delta\lambda + \dot{\lambda})\hat{\mathbf{p}})\right)\,, \tag{10}$$

once $\dot{\lambda}$ is known.[1] The additional equation, necessary to compensate the new unknown $\dot{\lambda}$, which proves to be computationally efficient and furnishes very simple results, can be written as

$$\Delta\mathbf{u}\cdot\mathbf{K}\dot{\mathbf{u}} = 0\,, \tag{11}$$

which forces the *orthogonality* between $\Delta\mathbf{u}$ and $\dot{\mathbf{u}}$ in the scalar product defined by the stiffness matrix $\mathbf{K}$. From (9) and (11), simple calculations gives

$$\dot{\lambda} = \frac{\hat{\mathbf{u}}\cdot\mathbf{r}}{\hat{\mathbf{u}}\cdot\hat{\mathbf{p}}}\,, \tag{12}$$

being the rest $\mathbf{r} = \mathbf{s}[\mathbf{u}_i + \Delta\mathbf{u}] - (\mathbf{p}_0 + (\lambda_i + \Delta\lambda)\hat{\mathbf{p}})$ and $\hat{\mathbf{u}} = \mathbf{K}[\mathbf{u}_i]^{-1}\hat{\mathbf{p}}$. Successively, by using (10), we can compute the correction $\dot{\mathbf{u}}$ for the Newton's extrapolation $\Delta\mathbf{u}$.

[1] The stiffness matrix $\mathbf{K}$ is now computed in $\mathbf{u}_i + \Delta\mathbf{u}$.

Table 1
Data, in S.I. units, used for numerical simulations of the pantographic beam reported in Fig. 1.

L	α	n_{uc}	a	b	c	d
1.05	$\pi/4$	21	10,000	10	1	0

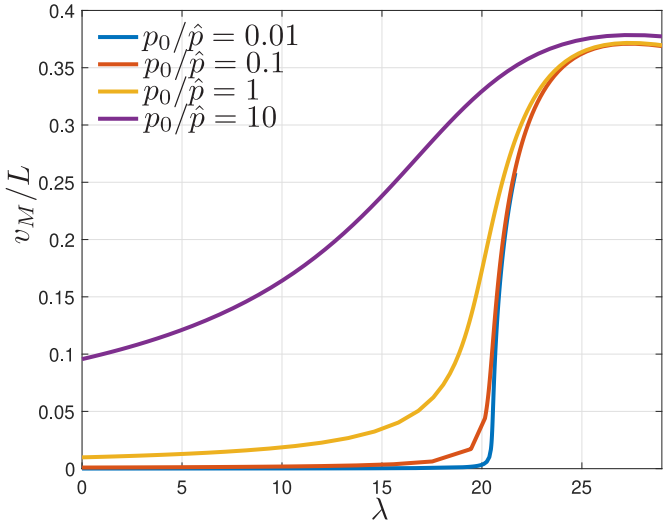

Fig. 2. Equilibrium paths of the pantographic beam reported in Fig. 1 changing the imperfection size: dimensionless parameter λ and dimensionless vertical displacement v_M/L of the mid-point M.

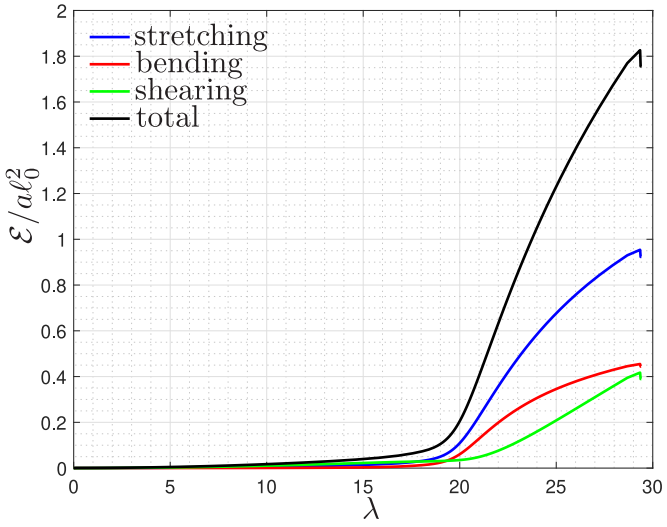

Fig. 3. Scaled strain energies versus λ. Stretching $\mathcal{E}_a$, bending $\mathcal{E}_b + \mathcal{E}_d$, shearing $\mathcal{E}_c$ contributions to the total strain energy $\mathcal{E}_a + \mathcal{E}_b + \mathcal{E}_c + \mathcal{E}_d$ ($n_{uc} = 21$, $a = 10,000$, $b = 10$, $c = 1$ and $d = 0$).

The algorithm briefly exposed here is simple but well-tailored to reconstruct complex equilibrium paths deriving from buckling problems also for complex structures such as pantographic beams, see [33]. Indeed, solving the Hencky model with the procedure sketched in the foregoing we can compute the equilibrium path for the considered pantographic beam. Numerical values employed for simulations are reported in Table 1.[2]

From these values and by varying the imperfection size, we computed the equilibrium paths shown in Fig. 2 obtained by plotting the dimensionless vertical displacement of the mid-point M *vs.* λ for the ratio $p_0/\hat{p} = 0.01 \ldots 10$. From this Figure, it can be easily estimated the value of the bifurcation load, *i.e.* approximatively more than 20 ($\hat{p} = 1$ in S.I. units).

We further plot in Fig. 3 the total strain energy, scaled by $a\ell_0^2$ ($\ell_0 = \sqrt{2}L/(2n_{uc})$), versus the dimensionless load parameter λ for the case $p_0/\hat{p} = 1$. In the same figure we also plot the contributions to the total strain energy, scaled again by the product

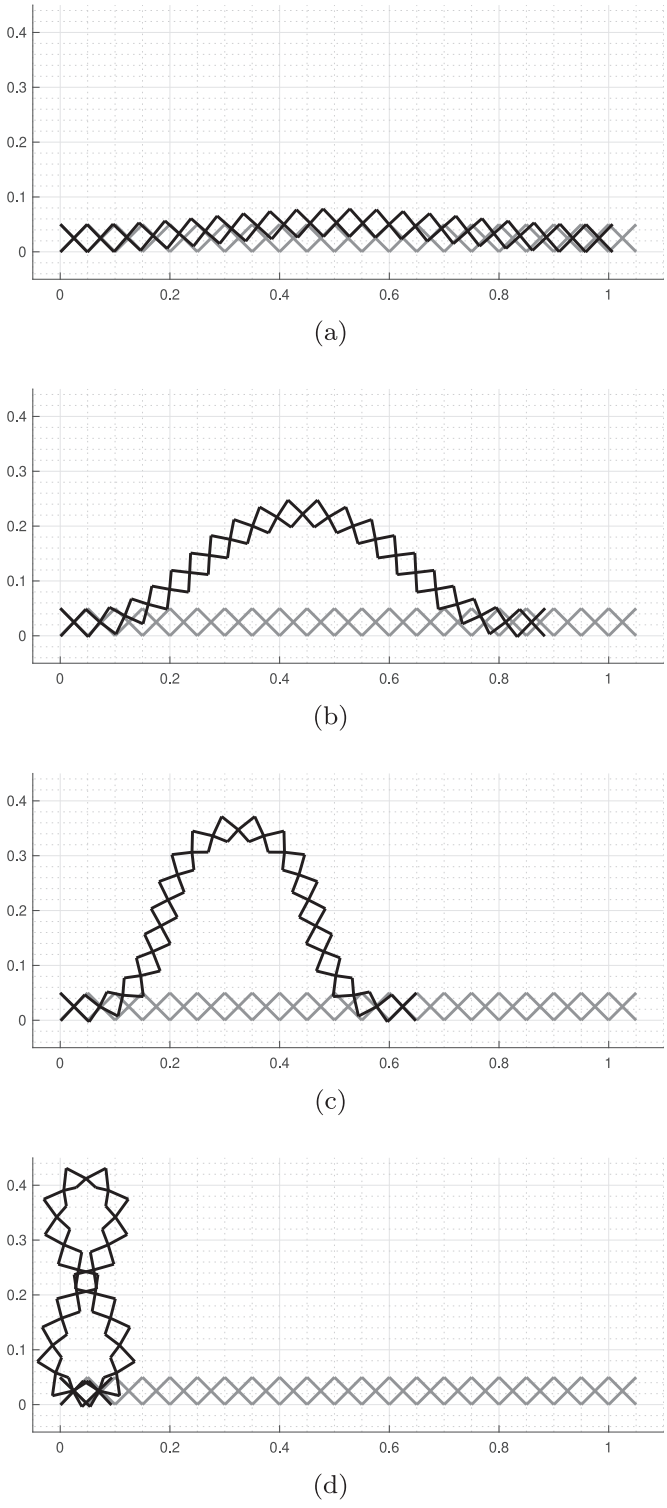

Fig. 4. Deformations for four equidistant values of λ (in terms of performed steps) for the case $p_0/\hat{p} = 1$.

[2] Here, we only consider the case of $\alpha = \pi/4$ but in [34] there are numerical simulations for different value of α.

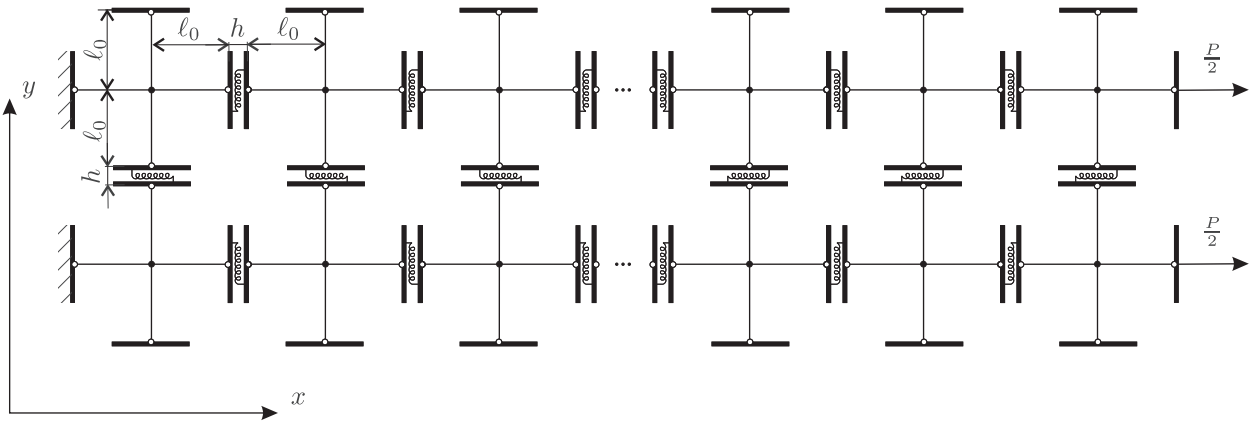

Fig. 5. Cross potent beam-like structure with sliders loaded by a force P.

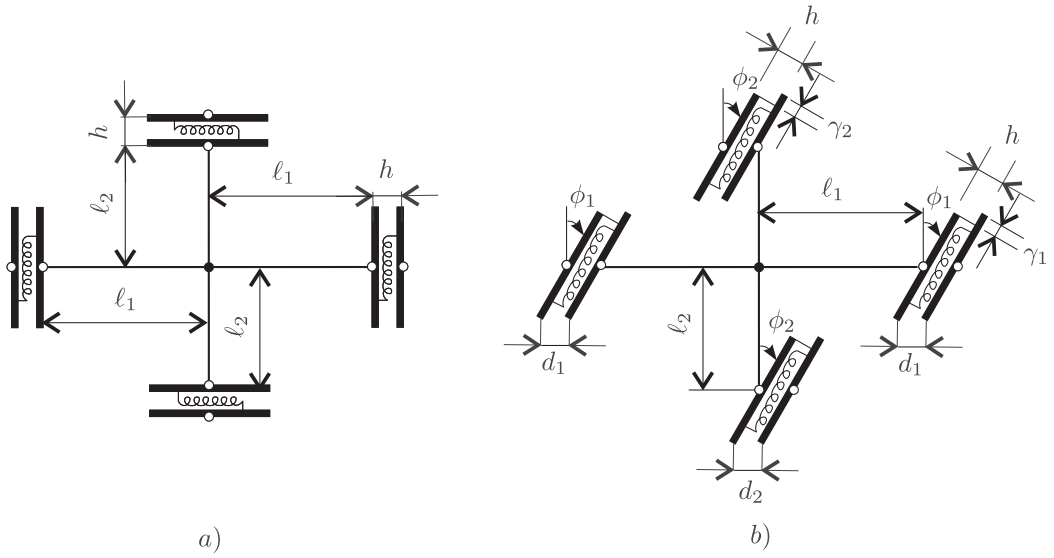

Fig. 6. a) Translational and b) rotational regime of deformations for the cross potent beam-like structure. Here ℓ_α are the actual lengths of bars, ϕ_α are the rotation angles of the sliders, $\gamma_\alpha = h\tan\phi_\alpha$ and $d_\alpha = h/\cos\phi_\alpha$, $\alpha = 1, 2$.

$a\ell_0^2$, as distinguished in stretching, bending and shearing contributions. We clearly distinguish two distinct mechanical behaviors separated, approximatively, by the value of the bifurcation load.

Finally, always for the case $p_0/\hat{p} = 1$, we plot in Fig. 4 the current configuration of the system for four equidistant values of λ (in terms of performed steps). We note the eight-form of the final deformation. We remark that this form is admissible since the numerical code used for the performed simulations permits the overlapping of the pantographic beam elements. From the physical point of view such deformations may occur also due to initial imperfections in considered structure. The latter may result in "almost" in-plane deformations but not exactly in-plane ones.

3. Beam-lattice with sliders

Another example of non-trivial buckling behaviour corresponds to lattice structures with sliders. Let us consider, in the $x - y$ plane, a long beam consisting of $2n$ elastic cells connected to each other through sliders, see Fig. 5. The left end of the beam is fixed whereas the right end is loaded by extensional net force P. Each cell consists of four elastic extensible bars of length ℓ_0 and of stiffness a which are rigidly connected in a central elastic hinge. Each bar ends by a slider of constant thickness h which consists of two rigid bars connected through a shear springs of stiffness c as in [35]. Sliders can rotate with respect to connected elastic bars. So the shape of the cells is similar to a cross potent. The initial length of the beam is $L = 2n\ell_0 + (n-1)h$ whereas its width is $4\ell_0 + h$. Let us note that a two beams structure with a slider was proposed in [24] in order to demonstrate the phenomena of instability under tension. In what follows we show that similar behaviour we get also for the lattice discussed here.

Each cell can possess at least two regimes of deformation. The first one is a tension/compression along bars, that is along x-, y-directions, see Fig. 6a, whereas the second one relates to a rotation of sliders, see Fig. 6b. For brevity we call these regimes translational and rotational, respectively. Note that for the rotational regime extension/compression of elastic bars is also admissible.

Considering elongation of the beam in x-direction and assuming uniform deformations we get two kinematic variables that are $\varepsilon_1 = (\ell_1 - \ell_0)/\ell_0$ and ϕ_1, whereas $\varepsilon_2 \equiv (\ell_2 - \ell_0)/\ell_0 = 0$ and $\phi_2 = 0$. With this assumption the total energy of the beam is given by the formula

$$\mathcal{E} = \mathcal{E}(\varepsilon, \phi) = 2na\varepsilon_1^2 + (n-1)\frac{c}{h^2}\gamma_1^2 - Pu, \tag{13}$$

where

$$\gamma_1 = h\tan\phi_1,$$

$$u = 2\ell_0 n\varepsilon_1 + (n-1)\frac{h}{\cos\phi_1} - (n-1)h$$

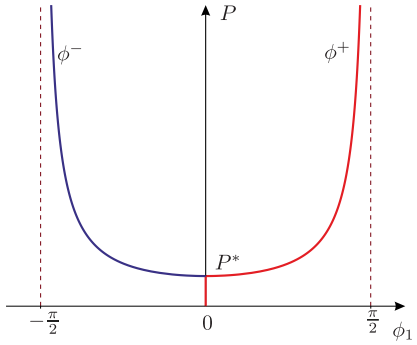

Fig. 7. Cross potent beam-like structure: rotation angle ϕ_1 *vs.* tensile force P.

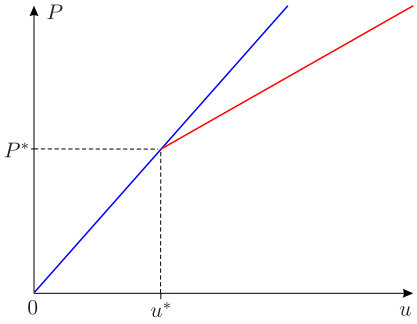

Fig. 8. Cross potent beam-like structure: tensile force P *vs.* displacement u.

are shear displacement in the sliders and the displacement of the right end of the beam, respectively.

The equilibrium conditions follow from the stationarity of $\mathcal{E}$ that is from the relations

$$\frac{\partial \mathcal{E}}{\partial \varepsilon} = 0, \quad \frac{\partial \mathcal{E}}{\partial \phi_1} = 0.$$

From the latter we get two equations

$$4na\varepsilon_1 - 2\ell_0 nP = 0, \tag{14}$$

$$(n-1)h\tan\phi_1 \frac{P\cos\phi_1 - 2c}{\cos^2\phi_1} = 0. \tag{15}$$

From (14) we get $\varepsilon_1 = P\ell_0/2a$. As ϕ_1 is in the range $-\pi/2 \le \phi_1 \le \pi/2$, Eq. (15) has the trivial solution $\phi_1 = 0$ and two non-trivial ones

$$\phi_1 = \phi^{\pm} \equiv \pm \arccos\frac{2c}{P}. \tag{16}$$

The non-trivial solutions exist when the applied force exceeds the critical value $P \ge P^*$, where $P^* = 2c$.

So the trivial solution corresponds to the translational deformations as in Fig. 6a, whereas non-trivial solutions relate to Fig. 6b. Dependence of ϕ_1 on P is given in Fig. 7. Note that it has a typical form of a postbuckling behaviour, see, *e.g.*, [19–21]. The loading curve is presented in Fig. 8. In the range $0 \le P \le P^*$ we have only trivial solution with $\phi_1 = 0$, whereas for $P > P^*$ there exists the rotational regime with ϕ_1. Note that both solutions $\phi^{\pm}$ correspond to the same loading curve shown in Fig. 8 as the red solid line. Here $u^* = 2n\ell_0^2 P^*/2a$.

Let us note that the here observed rotational instability is similar to one discussed in [24,25] for structures with sliders. On the other hand, it is different from the case of simple nonlinear elastic materials. Indeed, considering in-plane deformations of an elastic bar under tension within the nonlinear elasticity, in [36] it was proven that the bifurcation points, if exist, lie on a declined branch of the loading curve. Here we have the bifurcation point (u^*, P^*) on inclined loading line. So a continuum limit of the considered structure with sliders cannot be the Cauchy continuum. Again, one can see that a model with enriched kinematics may possess more complex buckling.

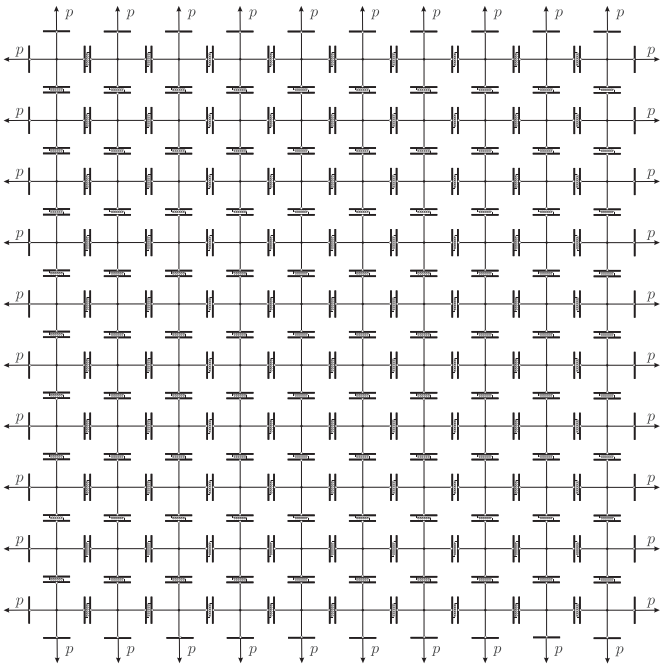

Fig. 9. Uniform extension of the $n \times n$-lattice with sliders, $p = P/n$, $n = 10$.

The here considered lattice with sliders demonstrates also the buckling under uniform in-plane tension. Indeed, let us consider a $n \times n$ lattice loaded by the force P/n as shown in Fig. 9 for $n = 10$. Here we have $\varepsilon_1 = \varepsilon_2$, $\ell_1 = \ell_2$ and the energy of the lattice coincides with (13) up to a constant factor. So we have here the bifurcation under uniform in-plane tension.

Let us note that solutions ϕ^- and ϕ^+ are equivalent as they correspond to the same value of the cell energy. So for $m \times n$-lattice with sliders we have 2^{mn} possible rotated states after bifurcation. In other words, the multiplicity of the eigenvalue corresponding to the bifurcation is quite large, that makes computations more difficult.

4. Concluding remarks and future challenges

The two examples of beam-lattices metamaterials presented and discussed in the foregoing show peculiar buckling behaviour. We used the term enriched to indicate that the mechanical response, *i.e.* the equilibrium path, depends from a fixed number of parameters, *e.g.* the stiffnesses of the springs which define the beam-lattice metamaterial, which can be accurately tuned to have the desired mechanical response. Both the examples show how to the numerically-driven approach, for the first example, and mathematically-driven approach, for the second example, can be profitably used for metamaterials design.

Considering the buckling of beam-lattice metamaterials presented here we conclude that enriched kinematics of a pantographic beam or cross potent beam with sliders results also in more complex buckling behaviour which can also call *enriched*. In the case of structural mechanics the typical extension of the Euler formula sound as

$$P^* = kP_E^*,$$

where P_E^* is a "canonical" Euler's critical force and k is a factor accounting for boundary conditions, shear deformations, shortening

during loading and other phenomena [18,19,21]. Here this modification does not work, in general. Indeed, the buckling for the beam with slider occurs under tension and P_E^* does not exists in this case. For the pantographic beam we observe not only high level of deformations for springs [18], but also an "exotic" 8-shape mode of buckling, see Fig. 2.

Summarizing, we conclude that the buckling of beam-lattice metamaterials can be characterized by: *i)* large stretching, translations and rotations; *ii)* multiplicity of buckling modes; *iii)* possible bifurcation in unusual regimes, such as the buckling under tension or under bending [33]; *iv)* high sensitivity to geometrical and mechanical parameters of the structure. For example, with too soft pivots the pantographic beam can "escape" buckling through shortening.

Future challenges concerns: *i)* the extension of the two examples shown in the above to three-dimensional case; for the first one a well-grounded starting point is the three-dimensional beam model presented in [37], for the second one spatial structures consisting of cubic elastic cells with sliding contact should be developed; *ii)* the building of homogenized models capable to predict the mechanical behaviour in case of large deformations; *iii)* similar to the nonlinear elasticity [38,39] and to Cosserat continuum [40–42] the elastic stability theory should be developed also for micromorphic and strain-gradient media; *iv)* both examples discussed in the foregoing can be studied experimentally by means of simple compression tests (avoiding the out-of-plane buckling with a specific design, for example by considering a package of pantographic beams), using the capability of the new 3D printing technology and of the digital image correlation, see [16,17] and therein references for pantographic structures, conversely, cross potent beam-like structures require besides standard traction tests a preliminary accurate design above all for the sliders; *v)* the introduction of opportunely defined damaging law, such as depicted in [43,44], is surely interesting besides to be simply to code in an algorithm such as briefly sketched in this work.

Declaration of Competing Interest

The authors declare that they do not have any financial or non-financial conflict of interests.

Acknowledgement

V. A. E. gratefully acknowledges his appointment as a Visiting Research Professor at the University of Sassari, Department of Architecture, Design and Urban Planning, Italy, in 2019 during the course of this research.

Supplementary material

Supplementary material associated with this article can be found, in the online version, at doi:10.1016/j.mechrescom.2019.103458.

References

[1] L.J. Gibson, M.F. Ashby, Cellular Solids: Structure and Properties, Cambridge Solid State Science Series, 2nd ed., Cambridge University Press, Cambridge, 1997.
[2] N.A. Fleck, V.S. Deshpande, M.F. Ashby, Micro-architectured Materials: Past, Present and Future, in: Proceedings of the Royal Society A: Mathematical, Physical and Engineering Sciences, 466, 2010, pp. 2495–2516.
[3] A.S. Phani, M.I. Hussein, Dynamics of Lattice Materials, John Wiley & Sons, Chichester, 2017.
[4] L.R. Meza, G.P. Phlipot, C.M. Portela, A. Maggi, L.C. Montemayor, A. Comella, D.M. Kochmann, J.R. Greer, Reexamining the mechanical property space of three-dimensional lattice architectures, Acta Mater. 140 (2017) 424–432.
[5] L.R. Meza, S. Das, J.R. Greer, Strong, lightweight, and recoverable three-dimensional ceramic nanolattices, Science 345 (6202) (2014) 1322–1326.
[6] M.-S. Pham, C. Liu, I. Todd, J. Lertthanasarn, Damage-tolerant architected materials inspired by crystal microstructure, Nature 565 (7739) (2019) 305–311.
[7] Z. Vangelatos, V. Melissinaki, M. Farsari, K. Komvopoulos, C. Grigoropoulos, Intertwined microlattices greatly enhance the performance of mechanical metamaterials, Math. Mech. Solids 24 (8) (2019) 2636–2648.
[8] Z. Vangelatos, K. Komvopoulos, C. Grigoropoulos, Vacancies for controlling the behavior of microstructured three-dimensional mechanical metamaterials, Math. Mech. Solids 24 (2) (2018) 577–598.
[9] A. Gross, P. Pantidis, K. Bertoldi, S. Gerasimidis, Correlation between topology and elastic properties of imperfect truss-lattice materials, J. Mech. Phys. Solids 124 (2019) 577–598.
[10] R.S. Lakes, Foam structures with a negative Poisson's ratio, Science 235 (1987) 1038–1040.
[11] T.C. Lim, Auxetic Materials and Structures, Engineering Materials, Springer, Singapore, 2015.
[12] P. Trovalusci, A. Pau, Derivation of microstructured continua from lattice systems via principle of virtual works: the case of masonry-like materials as micropolar, second gradient and classical continua, Acta Mech. 225 (1) (2014) 157–177.
[13] Y. Rahali, I. Giorgio, J.F. Ganghoffer, F. dell'Isola, Homogenization à la Piola produces second gradient continuum models for linear pantographic lattices, Int. J. Eng. Sci. 97 (2015) 148–172.
[14] K.E. Nady, F.D. Reis, J.F. Ganghoffer, Computation of the homogenized nonlinear elastic response of 2D and 3D auxetic structures based on micropolar continuum models, Compos. Struct. 170 (2017) 271–290.
[15] H. Abdoul-Anziz, P. Seppecher, Strain gradient and generalized continua obtained by homogenizing frame lattices, Math. Mech. Complex Syst. 6 (3) (2018) 213–250.
[16] F. dell'Isola, P. Seppecher, M. Spagnuolo, E. Barchiesi, F. Hild, T. Lekszycki, I. Giorgio, L. Placidi, U. Andreaus, M. Cuomo, S.R. Eugster, A. Pfaff, K. Hoschke, R. Langkemper, E. Turco, R. Sarikaya, A. Misra, M. De Angelo, F. D'Annibale, A. Bouterf, X. Pinelli, A. Misra, B. Desmorat, M. Pawlikowski, C. Dupuy, D. Scerrato, P. Peyre, M. Laudato, L. Manzari, P. Göransson, C. Hesch, S. Hesch, P. Franciosi, J. Dirrenberger, F. Maurin, Z. Vangelatos, C. Grigoropoulos, V. Melissinaki, M. Farsari, W. Muller, B.E. Abali, C. Liebold, G. Ganzosch, P. Harrison, R. Drobnicki, L. Igumnov, F. Alzahrani, T. Hayat, Advances in pantographic structures: design, manufacturing, models, experiments and image analyses, Continuum Mech. Thermodyn. 31 (4) (2019) 1231–1282, doi:10.1007/s00161-019-00806-x.
[17] F. dell'Isola, P. Seppecher, J.J. Alibert, T. Lekszycki, R. Grygoruk, M. Pawlikowski, D.J. Steigmann, I. Giorgio, U. Andreaus, E. Turco, M. Gołaszewski, N. Rizzi, C. Boutin, V.A. Eremeyev, A. Misra, L. Placidi, E. Barchiesi, L. Greco, M. Cuomo, A. Cazzani, A. Della Corte, A. Battista, D. Scerrato, I. Zurba Eremeeva, Y. Rahali, J.-F. Ganghoffer, W. Muller, G. Ganzosch, M. Spagnuolo, A. Pfaff, K. Barcz, K. Hoschke, J. Neggers, F. Hild, Pantographic metamaterials: an example of mathematically driven design and of its technological challenges, Continuum Mech. Thermodyn. 31 (4) (2019) 851–884.
[18] S.P. Timoshenko, J.M. Gere, Theory of Elastic Stability, 2nd, McGraw-Hill, Auckland, 1963.
[19] M. Pignataro, N. Rizzi, A. Luongo, Stability, Bifurcation and Postcritical Behaviour of Elastic Structures, Elsevier, Amsterdam, 1991.
[20] S.S. Antman, Nonlinear problems of elasticity, Vol. 107 of Applied Mathematical Sciences, 2nd ed., Springer Science+Business Media, New York, 2005.
[21] Z.P. Bažant, L. Cedolin, Stability of Structures. Elastic, Inelastic, Fracture and Damage Theories, World Scientific Publishing, New Jersey, 2010.
[22] S.H. Kang, S. Shan, A. Košmrlj, W.L. Noorduin, S. Shian, J.C. Weaver, D.R. Clarke, K. Bertoldi, Complex ordered patterns in mechanical instability induced geometrically frustrated triangular cellular structures, Phys. Rev. Lett. 112 (9) (2014) 98701.
[23] K. Bertoldi, V. Vitelli, J. Christensen, M. van Hecke, Flexible mechanical metamaterials, Nat. Rev. Mater. 2 (11) (2017) 17066.
[24] D. Zaccaria, D. Bigoni, G. Noselli, D. Misseroni, Structures Buckling under Tensile Dead Load, in: Proceedings of the Royal Society A: Mathematical, Physical and Engineering Sciences, 467, 2011, pp. 1686–1700.
[25] D. Bigoni, N. Bordignon, A. Piccolroaz, S. Stupkiewicz, Bifurcation of Elastic Solids with Sliding Interfaces, in: Proceedings of the Royal Society A: Mathematical, Physical and Engineering Sciences, 474, 2018, p. 20170681.
[26] E. Turco, F. dell'Isola, A. Cazzani, N.L. Rizzi, Hencky-type discrete model for pantographic structures: numerical comparison with second gradient continuum models, Zeitschrift für Angewandte Mathematik und Physik 67 (85) (2016) 1–28.
[27] E. Turco, M. Golaszewski, A. Cazzani, N.L. Rizzi, Large deformations induced in planar pantographic sheets by loads applied on fibers: experimental validation of a discrete lagrangian model, Mech. Res. Commun. 76 (2016) 51–56.
[28] E. Turco, K. Barcz, M. Pawlikowski, N.L. Rizzi, Non-standard coupled extensional and bending bias tests for planar pantographic lattices. Part I: Numerical simulations, Zeitschrift Für Angewandte Mathematik Und Physik 67 (122) (2016) 1–16.
[29] E. Turco, K. Barcz, N.L. Rizzi, Non-standard coupled extensional and bending bias tests for planar pantographic lattices. Part II: Comparison with experimental evidence, Zeitschrift Für Angewandte Mathematik Und Physik 67 (123) (2016) 1–16.
[30] E. Turco, I. Giorgio, A. Misra, F. dell'Isola, King post truss as a motif for internal structure of (meta)material with controlled properties, R. Soc. Open Sci. (2017) 4171153.
[31] E. Turco, A. Misra, M. Pawlikowski, F. dell'Isola, F. Hild, Enhanced Piola–Hencky discrete models for pantographic sheets with pivots without deformation energy: numerics and experiments, Int. J. Solids Struct. 147 (2018) 94–109.

[32] E. Riks, The application of Newton's method to the problem of elastic stability, J. Appl. Mech. Trans. ASME 39 Ser. E (4) (1972) 1060–1065.
[33] E. Turco, E. Barchiesi, Equilibrium paths of Hencky pantographic beams in three-point bending problem, Mathematics and Mechanics of Complex System (2019) 1–20. (in press)
[34] E. Turco, M. Golaszewski, I. Giorgio, F. D'Annibale, Pantographic lattices with non-orthogonal fibres: experiments and their numerical simulations, Compos. Part B 118 (2017) 1–14.
[35] S. Casolo, Modelling in-plane micro-structure of masonry walls by rigid elements, Int. J. Solids Struct. 41 (13) (2004) 3625–3641.
[36] L.M. Zubov, A.N. Rudev, The instability of a non-linearly elastic beam under tension, J. Appl. Math. Mech. (PMM) 60 (5) (1996) 777–788.
[37] E. Turco, Discrete is it enough? The revival of Piola–Hencky keynotes to analyze three-dimensional *elastica*, Continuum Mech. Thermodyn. 30 (5) (2018) 1039–1057.
[38] R.W. Ogden, Non-Linear Elastic Deformations, Dover, Mineola, 1997.
[39] Y.B. Fu, R.W. Ogden, Nonlinear stability analysis of pre-stressed elastic bodies, Continuum Mech. Thermodyn. 11 (1999) 141–172.
[40] V.A. Eremeyev, L.M. Zubov, On the stability of elastic bodies with couple stresses, Mech. Solids 29 (3) (1994) 172–181.
[41] D.N. Sheydakov, H. Altenbach, Stability of inhomogeneous micropolar cylindrical tube subject to combined loads, Math. Mech. Solids 21 (9) (2016) 1082–1094.
[42] R.S. Lakes, Stability of Cosserat solids: size effects, ellipticity and waves, J. Mech. Mater. Struct. 13 (1) (2018) 83–91.
[43] E. Barchiesi, G. Ganzosch, C. Liebold, L. Placidi, R. Grygoruk, W.H. Müller, Out-of-plane buckling of pantographic fabrics in displacement-controlled shear tests: experimental results and model validation, Continuum Mech. Thermodyn. 31 (2019) 33–45.
[44] L. Placidi, A. Misra, E. Barchiesi, Simulation results for damage with evolving microstructure and growing strain gradient moduli, Continuum Mech. Thermodyn. 31 (2019) 1143–1163.